

## Electrical Double Layer Catalyzed Wet-Etching of Silicon Dioxide

Haitao Liu, Michael L. Steigerwald,\* and Colin Nuckolls\*

Department of Chemistry and the Columbia University Center for Electronics of Molecular Nanostructures,  
Columbia University, 3000 Broadway, New York, New York 10027

Received April 24, 2009; E-mail: mls2064@columbia.edu; cn37@columbia.edu

We show here that the electrical double layer can be used to pattern nanoscale trenches in silicon dioxide.

The ability to spatially modulate reaction kinetics lies at the heart of the photolithography process, in which a photochemically patterned film of photoresist is used to mask part of the wafer from reacting with the etchant. The resolution of the photolithography process is diffraction-limited. State-of-the-art lithography processes use 193 nm light to produce features as small as 45 nm; processes that use even shorter wavelengths face significant technological and economic challenges.<sup>1</sup> Here we show an alternate type of lithography where the electrical double layer around a carbon nanotube (CNT) can be used to create ultrasmall trenches in silicon dioxide.

The electrical double layer exists at the electrode–water interface. It plays an important role in many electrochemical and electrokinetic processes.<sup>2</sup> Within the electrical double layer, one polar (positive or negative) component of the electrolyte is preferentially accumulated both at the solid surface and in the diffuse layer, while the other polar component of the electrolyte is accordingly depleted in the same region. Such variations in the ion concentrations in principle can be used to spatially modulate the rate of chemical reactions. Thus, the electrical double layer can be used as a “mask” to transfer an existing pattern to a substrate. The ultimate resolution of this process is limited by the dimension of the electrical double layer, which is characterized by the Debye length. For an aqueous solution of a 1:1-type strong electrolyte at 25 °C, the Debye length can be estimated as

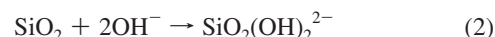
$$\frac{1}{\kappa} \approx \frac{0.30}{\sqrt{I}} \quad (1)$$

where  $1/\kappa$  is the Debye length in nanometers and  $I$  is the concentration of the electrolyte in moles per liter.<sup>3</sup> The thickness of the electrical double layer is smaller than 1 nm in a moderately concentrated ( $\sim 1$  M) solution of a strong electrolyte.

The electrical double layer exists not only on the surface of conducting materials but also on insulating ones. The adsorption of hydroxide ions on hydrophobic surfaces is of particular relevance to our current study. It has been known for decades that a hydrophobic surface acquires negative charges in pure water.<sup>4</sup> Recent studies have shown that this phenomenon is due to the *spontaneous* adsorption of hydroxide at the hydrophobic–water interface.<sup>5</sup> The exact mechanism is not fully understood. Molecular dynamics simulations have shown that water molecules restructure near the hydrophobic surface with the hydrogen atoms pointing toward the hydrophobic surface and the oxygen atoms pointing into the aqueous phase.<sup>6</sup> This ordered structure creates a huge dipole moment near the hydrophobic surface and presumably allows hydroxide ions to adsorb via dipole interactions and hydrogen bonding. Indeed, a recent electrochemical study suggested that the adsorbed  $\text{OH}^-$  forms a more ordered structure at the graphene–water interface than  $\text{H}_3\text{O}^+$  does.<sup>7</sup>

Because of the spontaneous hydroxide adsorption, pure hexadecane droplets acquire a  $\zeta$  potential of  $-120$  mV in a pH 9 solution.<sup>5</sup> The density of hydroxide at the hexadecane–water interface is  $\sim 0.3$  molecule/nm<sup>2</sup>.<sup>5</sup> The average hydroxide-to-hydroxide distance on the hexadecane surface is comparable to that in a  $\sim 0.3$  M hydroxide solution (i.e., the effective pH on the surface of hexadecane is  $\sim 14$ , in contrast to the pH of 9 in the solution). All of this information clearly suggests that the hydrophobic surface may significantly accelerate chemical reactions that involve hydroxide.

To experimentally verify this hypothesis, we studied the effect of the electrical double layer on the wet etching of silicon dioxide in a strong alkaline solution:



CNTs were chosen as the hydrophobic material. According to our hypothesis, the  $\text{SiO}_2$  near the electrical double layer of the CNTs should experience a higher effective concentration of hydroxide and be preferentially etched away to produce a nanoscale trench (Figure 1).

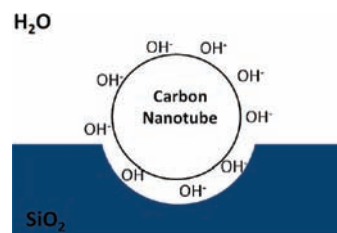


**Figure 1.** Adsorption of hydroxide ions at the CNT–water interface locally increases the rate of  $\text{SiO}_2$  etching.

Ultralong, aligned CNTs on a Si wafer (300 nm of thermal oxide) were grown using the chemical vapor deposition (CVD) method.<sup>8</sup> Our growth conditions produced both single-walled and multiwalled CNTs with diameters in the range 1–4 nm [Figure S1 in the Supporting Information (SI)]. After the growth, marks (50 nm of thermally evaporated Au with 5 nm of Cr or Ti as an adhesion layer) were patterned onto the wafer with electron-beam lithography. The CNTs were located relative to the mark by using a scanning electron microscope (SEM). The wafer was then treated with an aqueous solution of tetramethylammonium hydroxide,  $(\text{CH}_3)_4\text{N}^+\text{OH}^-$  (TMAH). In a typical reaction, the wafer was immersed in a 0.26 M solution of TMAH at 50 °C for 10 h (see the SI). The wafer was rinsed with deionized water after the etching and dried with a stream of nitrogen. We then used an atomic force microscope (AFM) to scan the area where the CNTs were known to exist before the etching. In most cases (see below), we observed nanoscale trenches instead of the CNTs. The shapes of the trenches closely resembled those of the original CNTs (Figure 2). The trenches survived an oxygen plasma treatment (250 mTorr  $\text{O}_2$ , 50 W, 45 s), showing that they were not an artifact due to the CNTs

or adsorbed organic materials. Replacing TMAH with NaOH gave qualitatively the same result (Figure S2). A typical trench was  $\sim 4\text{--}6$  nm deep and  $\sim 60$  nm wide in the opening.<sup>9</sup> CNT-guided formation of nanoscale SiO<sub>2</sub> trenches has been previously observed at 900 °C, following a carbon thermal reduction mechanism.<sup>10</sup> In contrast, our experiment was conducted close to room temperature and is compatible with the standard silicon microfabrication processes.

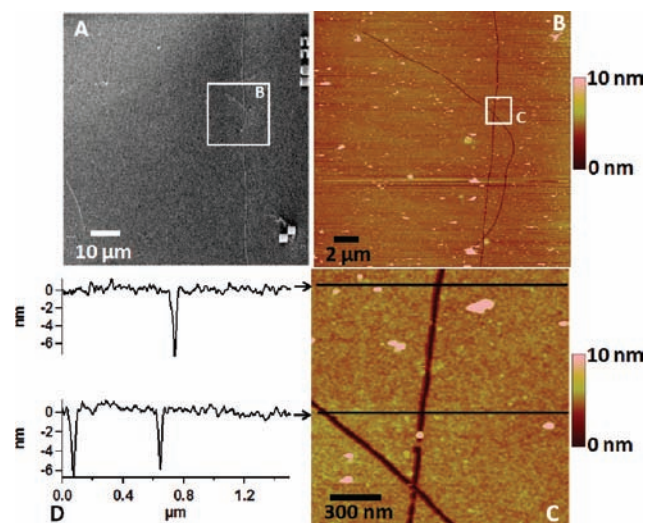


**Figure 2.** (A) SEM micrograph of a CNT taken before the etching. (B) Low- and (C) high-resolution AFM images of the same area taken after the etching. (D) Line profiles from (C).

Most of the trenches appeared to be free of CNTs, as observed using the SEM. Attempts to collect the Raman spectrum of CNTs from several trenches by using a micro-Raman setup were not successful. We also patterned pairs of electrodes onto several trenches. No sign of electrical connectivity was observed through these trenches (see the SI). However, in some rare cases, we were able to observe both the CNT and the trench in parallel (Figure S3). This was true especially for CNTs that were clamped down by the marks. We conclude that most of the CNTs were released from the wafer surface as the oxide beneath them was etched away. It is not clear when the CNTs were released from the oxide surface during the reaction.

The CNTs on the wafer were likely contaminated by the electron-beam resist [poly(methyl methacrylate), MW 950 kDa] that was used to pattern the marks. However, the trench formation was not a result of such contamination. To demonstrate this, we fabricated the marks with a shadow-masking process (see the SI). In this case, the CNTs were not in contact with any organic solvent or polymer before they were subjected to the etching process. We examined 13 of these clean CNTs after treating the wafer with TMAH. Among them, nine CNTs produced trenches while the other four did not.

Under our reaction conditions (0.26 M TMAH, 50 °C), the etching rate of bulk SiO<sub>2</sub> was measured to be 0.19 nm/h (see the SI). A typical trench obtained under these conditions grew at an average rate of  $\sim 0.5$  nm/h in the vertical direction. Thus, the silicon dioxide near the CNTs was etched 3 times faster than the bulk material. The diameter of the electrical double layer was 2–5 nm under our reaction conditions. The width of the trench at the opening

was  $\sim 60$  nm, which is much larger than the theoretical limit. We suspect that the CNTs are very mobile during the etching process, causing significant broadening of the trench.<sup>11</sup> One way to minimize the movement of the CNTs is to covalently attach them onto a base-resistant substrate and use this CNT-patterned substrate as a “stamp” to pattern the SiO<sub>2</sub>. In addition, the choice of the hydrophobic surface is not limited to CNTs. For example, a hydrophobic polymer film that is spin-coated onto SiO<sub>2</sub> and patterned by photolithography may be used to generate nanoscale trenches at the edges of the photolithography pattern.

In conclusion, we have shown that the electrical double layer can be exploited to spatially modulate the rate of chemical reactions. In particular, we have demonstrated that the electrical double layer around the CNTs accelerates the wet etching of SiO<sub>2</sub> by locally increasing the concentration of hydroxide. We emphasize that the use of the electrical double layer to modulate the reaction rate is not limited to ones involving hydroxide. By supplying an external bias to the electrode, ions other than hydroxide can be accumulated in the electrical double layer as well. Controlling the reaction kinetics at the nanoscale may open up new avenues for improving the resolution of existing photolithography methods and provide a route to new types of nanofluidic devices.<sup>12</sup>

**Acknowledgment.** We thank Professor Louis E. Brus and Dr. Jinyao Tang for helpful discussions. We acknowledge support from the Chemical Sciences, Geosciences, and Biosciences Division, Office of Basic Energy Sciences, U.S. DOE (DE-FG02-01ER15264), the DOE Basic Energy Sciences Program under FG02-98ER14861, the Nanoscale Science and Engineering Initiative of the NSF under Award CHE-0641523, and the New York State Office of Science, Technology, and Academic Research (NYSTAR). We used characterization facilities supported by the Columbia MRSEC under NSF Award DMR-02113574.

**Supporting Information Available:** Experimental details and Figures S1–S3. This material is available free of charge via the Internet at <http://pubs.acs.org>.

## References

- (1) International Technology Roadmap for Semiconductors, 2007 ed. <http://www.itrs.net/Links/2007ITRS/Home2007.htm> (accessed May 2009).
- (2) (a) Devanathan, M. A. V.; Tilak, B. V. K. S. R. *Chem. Rev.* **1965**, *65*, 635–684. (b) Parsons, R. *Chem. Rev.* **1990**, *90*, 813–826.
- (3) *Springer Handbook of Nanotechnology*; Bhushan, B., Ed.; Springer: Berlin, 2004; p 871.
- (4) (a) McCarty, L. S.; Whitesides, G. M. *Angew. Chem., Int. Ed.* **2008**, *47*, 2188–2207. (b) Beattie, J. K. *Lab Chip* **2006**, *6*, 1409–1411.
- (5) Beattie, J. K.; Djerdjev, A. M. *Angew. Chem., Int. Ed.* **2004**, *43*, 3568–3571.
- (6) Mamatkulov, S. I.; Khabibullaev, P. K.; Netz, R. R. *Langmuir* **2004**, *20*, 4756–4763.
- (7) Ang, P. K.; Chen, W.; Wee, A. T. S.; Loh, K. P. *J. Am. Chem. Soc.* **2008**, *130*, 14392–14393.
- (8) Zheng, L. X.; O’Connell, M. J.; Doorn, S. K.; Liao, X. Z.; Zhao, Y. H.; Akhador, E. A.; Hoffbauer, M. A.; Roop, B. J.; Jia, Q. X.; Dye, R. C.; Peterson, D. E.; Huang, S. M.; Liu, J.; Zhu, Y. T. *Nat. Mater.* **2004**, *3*, 673–676.
- (9) Because of the finite radius of the AFM tip, these measurements underestimate the true geometry of the trench.
- (10) Byon, H. R.; Choi, H. C. *Nat. Nanotechnol.* **2007**, *2*, 162–166.
- (11) It is also possible that the electrical double layer model, which was developed for the bulk surfaces, may not describe the nanoscale interface well.
- (12) Goldberger, J.; Fan, R.; Yang, P. D. *Acc. Chem. Res.* **2006**, *39*, 239–248.

JA90333S